





## **STATEMENT OF ORIGINALITY**

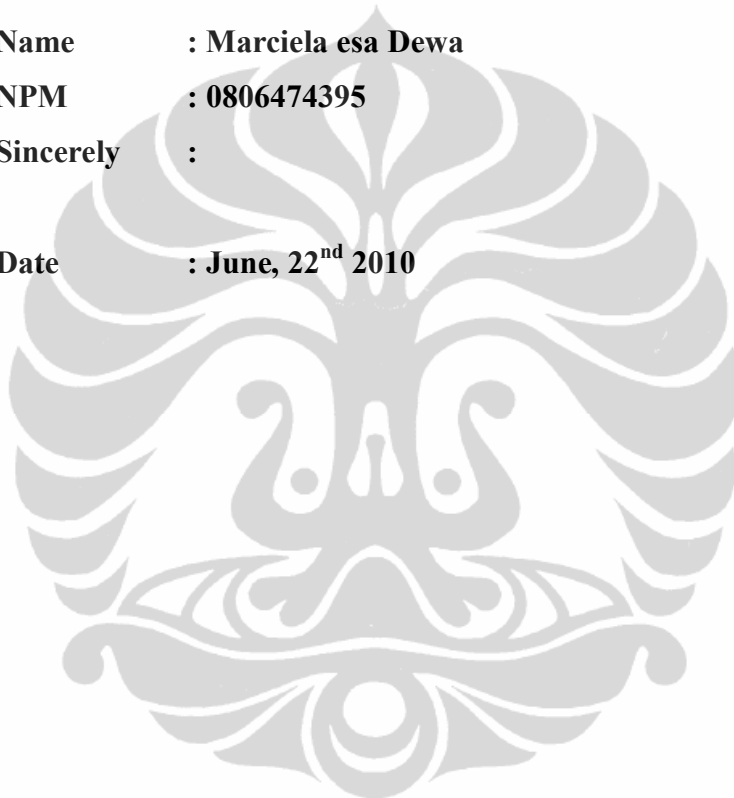
**This thesis has been made by me,  
and all the resources where the writer quote,  
has been correctly stated below**

**Name : Marciela esa Dewa**

**NPM : 0806474395**

**Sincerely :**

**Date : June, 22<sup>nd</sup> 2010**



## APPROVAL

This Thesis is made by,

Name : Marciela Esa DEWA

NPM : 0806474395

Program Study : Civil Engineering

Title : Collapse Process Due to Tunneling Erosion in Earth Dams: a Numerical Study

**Has been successfully maintain in front of the judge and fulfill as one requirement to obtain Master of Engineering, Civil Engineering Department, Faculty of Engineering, University of Indonesia.**

Supervisor : Prof. Dr. Ir. Irwan KATILI, DEA. ( )

State in : Depok

Date : June, 22<sup>nd</sup> 2010

## PREFACE

This research was carried out within the Geotechnical and Material Engineering group of the LTDS (Laboratory of Tribology and Dynamics of System) – *Geomatériaux du LTDS* of the Ecole Centrale de Lyon (ECL) in partnership with EDF (Energie de France) and Universitas Indonesia (Depok - Indonesia).

First of all, I would like to express my greatest gratitude with Mr. Jean-Jacques FRY and Mr. Eric VINCENS, to have supported me in the achievement of this work, for all the help which has allowed me to progress scientifically throughout my training course. Without them, this work would not have been carried out.

I would also thank Mr. Katili who gave me this opportunity to do this research in Lyon. Without him this work would not have been carried out. I also thank all the team for FTUI for me has to have formed until today.

I particularly thank all the team for LTDS G8:

- My “partner”, son, who accommodated me in “his office”, and for all his ideas and his conversations.
- Cécile, Hélène, and Nadège who shared their stories.
- Jean Patrick, Yoann, Alex, Francesco, Pierre-Yves, Pierre Adrien, Bruno, James, and Vuong who are always sportsmen (except for...☺) and amusing.
- Mrs Maryline Disero and Mrs Marie Chaze who helped me well for all the “administrative” problems and data-processing

I could not forget these moments. Thank you for these five unforgettable months of works.

Last but not the least, I would like to thank my family which gave me all the necessary support. “Bapak dan Ibu” which helped me spent difficult time much and especially their opinions which help me a lot. My three brothers, Satria, Putra, and Lasta which are always there for me. Finally for Hana (nip) which accompanied me throughout this work and her charming stories. Thank you very much!

# PAGE OF COPYRIGHT OF STATEMENT FOR PUBLICATION

## THESIS AS ACADEMIC NECESSITIES

---

As academic affiliate of University of Indonesia, authorized signature:

Name : Marciela esa DEWA

NPM : 0806474395

Major of Study : Master Degree

Department : Civil Engineer

Faculty : Engineer

Type of paper : Thesis

In order to support the development of science, the writer has agreed to give **Non-exclusive Royalty – Free Right** to University of Indonesia, according to the writers' academic paper entitled:

*COLLAPSE PROCESS DUE TO TUNNELING EROSION IN EARTH DAMS: A NUMERICAL STUDY*

Including the hardware (if necessary). Accompanying with the Non-exclusive Royalty – Free Right, University of Indonesia has the right to keep, format, manage in any form of database, treat and publish the writers' thesis as long as put the writers' name as the writer or creator and those who belong to the copyright owner.

Thus the certificate had been made by the means of fact:

Place : Depok

Date : June 22<sup>nd</sup>, 2010

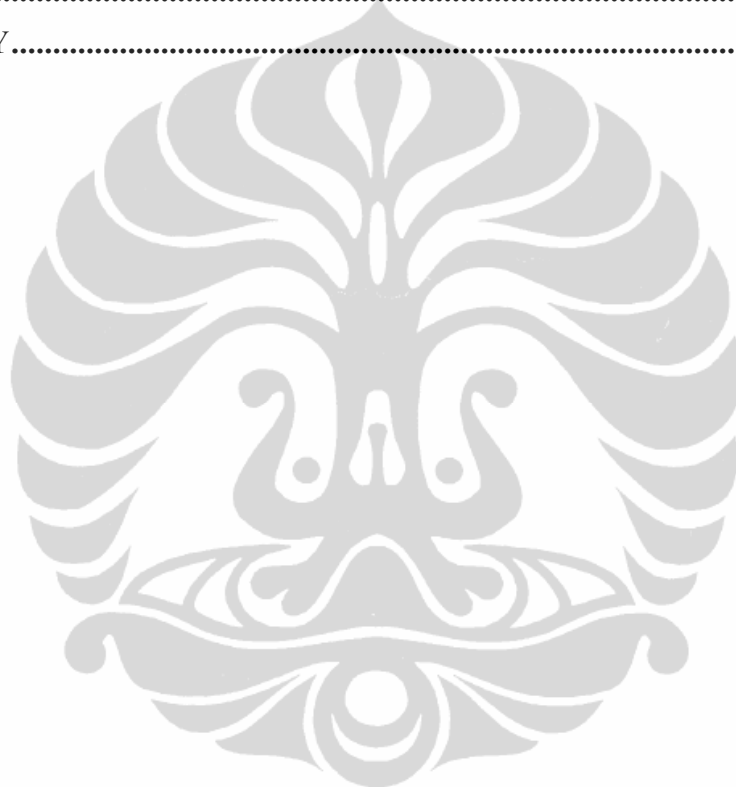
Sincere,

(Marciela esa DEWA)

# CONTENTS

STATEMENT OF ORIGINALITY .....	II
APPROVAL.....	III
PREFACE.....	IV
PAGE OF COPYRIGHT OF STATEMENT FOR PUBLICATION.....	V
CONTENTS.....	VI
LIST OF FIGURES.....	VIII
LIST OF TABLES.....	XI
ABSTRACT .....	XII
RESUME.....	XIII
<b>CHAPTER 1</b>	
<b>GENERAL PRESENTATION.....</b>	<b>1</b>
1.1    COLLAPSE OF CAVITIES: THE PHENOMENON.....	1
1.1.1 <i>Example of mode of rupture of a cavity</i> .....	2
1.1.2 <i>The case of Situ Gintung</i> .....	3
1.1.3 <i>Objectives of research</i> .....	4
1.2    CHARACTERISTICS OF THE SOIL .....	4
1.2.1 <i>Soil mechanics properties</i> .....	4
1.2.2 <i>Criterion of Mohr Coulomb</i> .....	5
1.2.3 <i>The classification of the soils</i> .....	6
<b>CHAPTER 2</b>	
<b>THE COLLAPSE OF CAVITIES: MODELLING.....</b>	<b>8</b>
2.1    THE STABILITY OF THE CAVITIES.....	8
2.1.1 <i>Observational approach</i> .....	8
2.1.2 <i>Analytical approach</i> .....	16
2.2    THE EXPANSION OF CAVITY .....	18
2.2.1 <i>The application of the expansion of cavities</i> .....	18
2.2.2 <i>Simplified calculation</i> .....	19
2.3    CROLET'S MODEL .....	20
<b>CHAPTER 3</b>	
<b>SPECIFIC STUDY OF THE COLLAPSE OF THE SOILS .....</b>	<b>23</b>
3.1    MODELING OF COLLAPSE.....	23
3.1.1 <i>Geometry</i> .....	23
3.1.2 <i>Rheological models</i> .....	25
3.1.3 <i>Numerical models</i> .....	30
3.2    CRITERIA OF COLLAPSE .....	38
3.2.1 <i>Analysis of Adimensional Parameters</i> .....	38
3.2.2 <i>Criteria of rupture</i> .....	38
3.2.3 <i>Cartography of the plastic zones</i> .....	43

3.2.4	<i>Cartography of vector of deformation.....</i>	<i>47</i>
<b>CHAPTER 4</b>		
<b>CRITICAL ANALYSIS OF THE NUMERICAL MODELLING.....</b>		<b>49</b>
4.1	ANALYZES WITH THE MODEL OF MOHR-COULOMB.....	49
4.1.1	<i>Earth dam - low height with circular cavity.....</i>	<i>49</i>
4.1.2	<i>Earth dam - low height with elliptic cavity.....</i>	<i>58</i>
4.1.3	<i>Earth dam - great height with circular cavity.....</i>	<i>71</i>
4.2	ANALYZE FOR MODEL OF MOHR COULOMB WITH SOFTENING.....	80
<b>CHAPTER 5</b>		
<b>CONCLUSION .....</b>		<b>93</b>
<b>BIBLIOGRAPHY .....</b>		<b>94</b>





## LIST OF FIGURES

Figure 1 Formation of a Cavity (LCPC INERIS) .....	3
Figure 2 Tragedy of Situ Gintung (seen above).....	3
Figure 3 Collapse of Gintung Situ.....	4
Figure 4 Mohr Circle (with mechanical properties of soil) .....	6
Figure 5 Diagrammatic cut of a cavity (Vachat's Study).....	9
Figure 6 Model of Piggott and Eynon .....	10
Figure 7 Model in cone (Piggott and Eynon).....	11
Figure 8 Model in triangle (Piggott and Eynon) .....	12
Figure 9 Model in rectangle (Piggott and Eynon).....	13
Figure 10 Results of the model of Piggott and Eynon.....	13
Figure 11 Vertical displacement according to Whittaker and Reddish.....	14
Figure 12 Model of subsidence by Whittaker and Reddish.....	14
Figure 13 Concept of induced fracturing.....	17
Figure 14 Iteration suggested by Abbas-Fayad on the analytical application of calculation ...	17
Figure 15 Transverse section of the conduit .....	23
Figure 16 Axisymmetric model with a circular cavity .....	24
Figure 17 Axisymmetric model with an elliptic cavity .....	24
Figure 18 Criterion of rupture of Mohr Coulomb in <i>FLAC</i> .....	26
Figure 19 Field used for the rule of flow .....	27
Figure 20 Radoucissant model.....	28
Figure 21 Approaches the model radoucissant in <i>FLAC2D</i> .....	29
Figure 22 Cut grid: compromise meanwhile and precision.....	31
Figure 23 Mohr Coulomb Model at the balance state.....	32
Figure 24 Mohr Coulomb Model with a circular cavity (here $r=1m$ ).....	32
Figure 25 Mohr Coulomb Model with an elliptic cavity (here, $a=5m$ ; $b=3m$ ).....	33
Figure 26 Model of great dimension ( $h=90m$ ; $r=54m$ ).....	35
Figure 27 Mechanical properties of the model radoucissant 1 .....	36
Figure 28 Mechanical properties of the model radoucissant 2 .....	37
Figure 29 Development of $\gamma^p$ during the creation of a cavity (value obtained with $r=5m$ ; $C=100kPa$ ).....	40
Figure 30 Development of $\gamma^p$ during the creation of a cavity with total rupture (value obtained with $r=5m$ ; $C=80kPa$ ) .....	42
Figure 31 Maximum coefficient of Reduction, taken of a curve $\gamma^p$ - R.....	43
Figure 32 Evolution of the index of plasticity .....	46
Figure 33 Evolution of the vectors speed .....	48
Figure 34 Mohr Coulomb Model with circular cavity ( $r=1m$ ).....	49

Figure 35 Mohr Coulomb Model with circular cavity ( $r=5m$ ) .....	50
Figure 36 Mohr Coulomb Model with circular cavity ( $r=9m$ ) .....	50
Figure 37 Comparison between the Mohr Coulomb Model and circular cavity .....	51
Figure 38 Presentation of $\gamma_p$ with total rupture, circular model MC cavity ( $r=5m$ ; $C=80kPa$ ) .....	52
Figure 39 Index of plasticity of the Mohr-Coulomb model in low height ( $r=5m$ , $Cu=80kPa$ ) .....	53
Figure 40 Vectors speed of the Mohr Coulomb Model in low height ( $r=5m$ , $Cu=80kPa$ ) .....	53
Figure 41 Zoom of the vectors speed of the Mohr Coulomb Model in low height ( $r=5m$ , $Cu=80kPa$ ) .....	54
Figure 42 Index of plasticity for the basic model (Mohr-Coulomb, $r=5m$ , $Cu=55kPa$ ).....	55
Figure 43 Displacement in Y of the Mohr Coulomb Model in low height ( $r=5m$ , $Cu=55kPa$ ) .....	56
Figure 44 Displacement in X of the Mohr Coulomb Model in low height ( $r=5m$ , $Cu=55kPa$ ) .....	56
Figure 45 Vectors speed of the Mohr Coulomb Model in low height ( $r=5m$ , $Cu=55kPa$ ) .....	57
Figure 47 Model of Mohr Coulomb with an elliptic cavity ( $a=5m$ $b=1m$ ).....	58
Figure 46 Mode of rupture during the widening of a conduit.....	58
Figure 48 Model of Mohr Coulomb with an elliptic cavity ( $a=5m$ $b=3m$ ).....	59
Figure 49 Presentation of $\gamma_p$ , elliptic model MC cavity ( $a=5m$ $b=1m$ ; $C=80kPa$ ).....	60
Figure 50 Presentation of $\gamma_p$ , elliptic model MC cavity ( $a=5m$ $b=3m$ ; $C=80kPa$ ).....	61
Figure 51 Vectors of speed, model MC with elliptic cavity ( $a=5m$ , $b=1m$ , $Cu=80kPa$ ) .....	61
Figure 52 Vectors of speed refined, model MC with elliptic cavity ( $a=5m$ , $b=1m$ , $Cu=80kPa$ ) .....	62
Figure 53 Vectors of speed, model MC with elliptic cavity ( $a=5m$ , $b=3m$ , $Cu=80kPa$ ) .....	62
Figure 54 Vectors of speed refined, model MC with elliptic cavity ( $a=5m$ , $b=3m$ , $Cu=80kPa$ ) .....	63
Figure 55 Index of plasticity, model MC with elliptic cavity ( $a=5m$ , $b=1m$ , $Cu=80kPa$ ) .....	63
Figure 56 Index of plasticity, model MC with elliptic cavity ( $a=5m$ , $b=3m$ , $Cu=80kPa$ ) .....	64
Figure 57 Comparison with different form of the geometry of cavity ( $C_{ref}=1300kPa$ ) .....	65
Figure 58 Index of plasticity, model MC with elliptic cavity ( $a=5m$ , $b=1m$ , $Cu=40kPa$ ) .....	65
Figure 59 Index of plasticity, model MC with elliptic cavity ( $a=5m$ , $b=3m$ , $Cu=55kPa$ ) .....	66
Figure 60 Comparison with different form of the geometry of cavity (flattened model; $C_{ref}=1300kPa$ ).....	66
Figure 61 Presentation of $\gamma_p$ , model MC with elliptic cavity ( $a=1m$ $b=5m$ ; $C=90kPa$ ) .....	67
Figure 62 Vectors of speed, model MC with elliptic cavity ( $a=1m$ , $b=5m$ , $Cu=90kPa$ ) .....	68
Figure 63 Index of plasticity, model MC with elliptic cavity ( $a=1m$ , $b=5m$ , $Cu=90kPa$ ) .....	68
Figure 64 Presentation of $\gamma_p$ , elliptic model MC cavity ( $a=1m$ $b=3m$ ; $C=90kPa$ ).....	69
Figure 65 Vectors of speed, Model MC with elliptic cavity ( $a=3m$ , $b=5m$ , $Cu=90kPa$ ).....	69
Figure 66 Index of plasticity, Model MC with elliptic cavity ( $a=3m$ , $b=5m$ , $Cu=90kPa$ ).....	70

Figure 67 Comparison between number of stability and various models .....	71
Figure 68 Comparison of the number of stability based in cohesion limits (model of 10m, 30m, 90m) .....	73
Figure 69 Comparison of the number of stability based in ultimate cohesion (model of 10m, 30m, 90m) .....	74
Figure 70 Value $\gamma_p$ refined Model MC great height ( $h=30m, r=27m, C_u=700kPa$ ) ( $\gamma_{pmax} = 50\%$ ).....	75
Figure 71 Value $\gamma_p$ refined and zoomée - Model MC great height ( $h=90m, r=27m, C_u=850kPa$ ) ( $\gamma_{pmax} = 5\%$ ).....	75
Figure 72 Vectors of displacement models great height (MC, $h=30m, r=27m, C_u=700kPa$ ).....	76
Figure 73 Refined vectors of displacement model MC great height ( $h=90m, r=27m, C_u=850kPa$ ) .....	76
Figure 74 Index of plasticity model MC, great height ( $h=30m, r=27m, C_u=700kPa$ ) .....	77
Figure 75 Index of plasticity model MC, great height ( $h=90m, r=27m, C_u=850kPa$ ) .....	77
Figure 76 Comparison models great height with circular cavity of 27 m (MC).....	78
Figure 77 Comparison models great height with circular cavity of 18 m (MC).....	78
Figure 78 Comparison models great height with circular cavity of 9 (MC).....	79
Figure 79 Comparison models great height with circular cavity of 1 (MC).....	79
Figure 80 Result of the model radoucissant 1 & 2, and Mohr Coulomb (circle, $r=5m$ ) ( $C_{ref}=5000kPa$ ) .....	82
Figure 81 Value $\gamma_p$ - Model Radoucissant 1 ( $h=10m, r=5m, C_u=80kPa$ ) .....	83
Figure 82 Value $\gamma_p$ refined - Model Radoucissant 1 ( $h=10m, r=5m, C_u=80kPa$ ).....	83
Figure 83 Value $\gamma_p$ - Model Radoucissant 2 ( $h=10m, r=5m, C_u=70kPa$ ) .....	84
Figure 84 Value $\gamma_p$ refined - Model Radoucissant 2 ( $h=10m, r=5m, C_u=70kPa$ ).....	84
Figure 85 Displacement in X model radoucissant 1 ( $h=10m, r=5m, C_u=80kPa$ ) .....	85
Figure 86 Displacement in Y model radoucissant 1 ( $h=10m, r=5m, C_u=80kPa$ ) .....	85
Figure 87 Displacement in X model radoucissant 2 ( $h=10m, r=5m, C_u=70kPa$ ) .....	86
Figure 88 Displacement in Y model radoucissant 2 ( $h=10m, r=5m, C_u=70kPa$ ) .....	86
Figure 89 Vectors of model displacement radoucissant 1 ( $h=10m, r=5m, C_u=80kPa$ ).....	87
Figure 90 Zoom of Vectors of displacement model radoucissant 1 ( $h=10m, r=5m, C_u=80kPa$ ).....	87
Figure 91 Vectors of displacement model radoucissant 2 ( $h=10m, r=5m, C_u=70kPa$ ).....	88
Figure 92 Index of plasticity model radoucissant 1 ( $h=10m, r=5m, C_u=80kPa$ ) .....	88
Figure 93 Index of plasticity model radoucissant 2 ( $h=10m, r=5m, C_u=70kPa$ ) .....	89
Figure 94 Comparison of the number of stability (all models; ultimate cohesion) .....	90
Figure 95 Comparison of the number of stability for the model in low height (ultimate cohesion) .....	91
Figure 96 Comparison of the number of stability for the model in great height (ultimate cohesion) .....	91

## LIST OF TABLES

Table 1 Various types of collapse .....	1
Table 2 Non-cohesive soils and cohesive soils: characteristics.....	7
Table 3 Soil mechanics properties.....	7
Table 4 Mohr Coulomb Model with a circular cavity in low height.....	31
Table 5 Mohr Coulomb Model with elliptic cavity.....	32
Table 6 Mohr Coulomb Model great height .....	34
Table 7 Model radoucissant 1 with a circular cavity.....	35
Table 8 Model radoucissant 2 with a circular cavity.....	36
Table 9 Result of the Mohr Coulomb Model with circular cavity.....	50
Table 10 Result of the Model of Mohr Coulomb with an elliptic cavity ( $C_u=1300kPa$ ) .....	59
Table 11 Mohr Coulomb Model in great height .....	72
Table 12 Number of stability based in cohesion limits (height of the model of 10m).....	72
Table 13 Number of stability based in cohesion limits (height of the model of 30m).....	72
Table 14 Number of stability based in cohesion limits (height of the model of 90m).....	72
Table 15 Number of stability based in ultimate cohesion (height of the model of 10m).....	73
Table 16 Number of stability based in ultimate cohesion (height of the model of 30m).....	73
Table 17 Number of stability based in ultimate cohesion (height of the model of 90m).....	73
Table 18 Model Radoucissant 1 (height of 10m) ( $C_{ref}=5000kPa$ ) .....	80
Table 19 Model Radoucissant 2 (height of 10m) ( $C_{ref}=5000kPa$ ) .....	80
Table 20 Model Radoucissant 1 (height of 90m) ( $C_{ref}=5000kPa$ ) .....	80
Table 21 Model Radoucissant 2 (height of 30m) ( $C_{ref}=5000kPa$ ) .....	81
Table 22 Model Radoucissant 2 (height of 90m) ( $C_{ref}=5000kPa$ ) .....	81

## **ABSTRACT**

Internal Erosion initiated by water movement along channels called tunnel erosion, often crack or defect the dam's structure. It is one of the main causes of water structure's (dams, dikes, etc.) collapse. This phenomenon can be divided into 3 phases, tunnelling, collapse, and the opening of the channel inside the dam [1]:

- "Tunnelling" transport large quantities of particles due to the hydraulic gradient. It's happen fast in a preferential path especially in some point of dam structure's weaknesses.
- The gradual collapse of the roof of tunnel erosion allows the expansion of the channel.
- The opening of the channel is started after the collapse of the channel by tunnel erosion.

Research has been done to explain the phenomenon of collapse, but there are still questions, including the formulation, phase, and form of the rupture. Moreover, the equation used is not always adapted to the various cases of the soil. Research by Hunt and Hanson showed the different phases of a dam collapse with a rate of expansion of a hole driven only by the constraint of shearing.

Through this numerical study, we find that their hypothesis is not correct, because there are other parameters that affect this phenomenon and also the effect of traction force. The study is simplified by modelling an earthen dam with a given cavity; where the undrained cohesion is controlled to see at which value of cohesion the fracture achieved. This simplification is the opposite in the real case, where the cohesion is fixed but the cavity expands. We find that the collapse of the earthen dam because of the tunnel erosion occurs in two stages: the arching effect in the channel across the dam that makes vertical sag then collapse, and the expansion of the channel which is inclined more like a slope. The high of the dam and the form of the "tunnel" cavity also influenced the failure mode.

Keyword: Internal Erosion, Collapse, Numerical Study, Tunnelling.

## Résumé

L'érosion interne dans un conduit dit « renard », résulte de l'infiltration d'eau souvent une fissure où un défaut à travers le corps du barrage. Elle est l'une des causes principales de ruptures hydrauliques (barrages, digues, etc.). Ce phénomène peut être décomposé en 3 phases, la phase de renard, l'effondrement, et la phase de brèche [1] :

- La phase de renard est à l'origine du transport des grandes quantités de particules à cause de la présence d'un gradient hydraulique. Celle-ci se fait rapidement dans un cheminement préférentiel le long duquel sont répartis un certain nombre des points faibles.
- L'effondrement progressif du toit du renard permet l'agrandissement du conduit.
- La phase de brèche est atteinte lors de la rupture totale du renard.

Des recherches ont été faites pour expliquer le phénomène d'effondrement, mais il reste encore des interrogations, notamment sur la forme de la rupture. Par exemple, l'équation utilisée n'est pas toujours adaptée aux différents cas du sol. Le travail de *Hunt et Hanson* a montré les différentes phases de rupture d'un barrage dont le taux d'élargissement d'une brèche est piloté uniquement par la contrainte de cisaillement.

Par cette étude numérique, nous trouvons que son hypothèse n'est pas correcte, auto il y a d'autres paramètres qui jouent sur ce phénomène et notamment la résistance à la traction du sol. L'étude réalisée est simplifiée par un barrage en terre avec une cavité donnée, où sa cohésion non drainée est diminuée pour voir à quelle valeur de cohésion on atteint la rupture. Ce qui est le contraire du cas réel où la cohésion est fixe mais la cavité s'agrandit. Nous trouvons que l'effondrement du barrage en terre à cause du renard se produit en deux temps : l'effet de voûte dans un conduit qui fait une affaissement vertical puis l'agrandissement de la brèche par formation d'un talus. La hauteur du barrage et la cohésion du sol influencent aussi le mode de rupture.

Mot Clé: Etude Numérique, L'érosion interne, L'effondrement, Renard.